Journal of Engineering and Technological Advances (JETA)
https://jeta.segi.edu.my/index.php/segi
2024 Vol. 9 No. 1

ENHANCING THE PERFORMANCE OF SOLAR TOWER POWER PLANTS USING AN AUXILIARY HEAT SOURCE

[1]Yazdi, M.H.[*], [1]Mahrooghi, A., [1]Zarandi, O.

[1]New Energy Research Group, New Materials Technology and Processing Research Center, Department of Mechanical Engineering, Neyshabur Branch, Islamic Azad University, Neyshabur 9319975853, Iran

* Corresponding Author: mohammadhossein.yazdi@gmail.com

Received: 16 March 2024; Accepted: 18 June 2024; Published: 30 June 2024

doi: 10.35934/segi.v9i1.110

Highlights:

- *To design a solar tower power plant that ensures uninterrupted electricity production, allowing for continuous generation even during nighttime hours.*
- *To simulate and numerically evaluate the thermal analysis of a hybrid solar chimney system using an auxiliary heat source.*
- *To enhance the performance of hybrid solar tower power plants for clean energy generation.*

Abstract: The solar tower power plant represents a cutting-edge solar thermal system designed to harness clean solar energy for electricity generation. Due to its abundant availability and cost-effectiveness, this technology has garnered significant interest recently. Solar power, as one of the most promising renewable energy sources, offers a sustainable alternative to fossil fuels, contributing to a reduction in greenhouse gas emissions and dependence on non-renewable energy resources. However, a major challenge lies in the plant's low efficiency and its inability to generate electricity during nighttime, cloudy weather, or rainfall. To tackle this challenge, our approach involves designing a solar tower power plant that integrates an external heat source to complement solar energy and ensure uninterrupted electricity production. This integration not only enhances the reliability of the power supply but also maximizes the utilization of renewable energy resources. The collector, a crucial component of the solar tower power plant, accounts for a significant portion of both construction costs and energy loss. Improving the collector's performance is therefore essential for enhancing the overall efficiency and economic viability of the plant. In this project, a novel collector design is proposed that not only heats the air under the collector through solar radiation but also utilizes an auxiliary heat source to further raise the air temperature. This increase in temperature accelerates air flow, which in turn enhances turbine rotation and consequently boosts electricity generation.

Keywords: solar tower power plant; renewable energy; thermal systems; solar collector; heat and mass transfer

1. Introduction

Solar chimney power plants are systems that harness solar energy to generate electricity. These systems consist of three main components: the solar air collector, the chimney, and the power generation unit, which includes a wind turbine and generator. The solar air collector is generally circular and consists of a transparent canopy and an absorber medium (usually natural ground). The gap between the canopy and the ground facilitates air movement. The chimney is installed at the center of the collector, and wind turbines are located at the base of the chimney. Solar rays penetrate through the canopy and are absorbed by the ground, which in turn heats the air. Due to the density difference, warm air flows into the chimney and rotates the turbine, generating electricity through the generator. Despite their advantages, such as low maintenance costs, high reliability, and minimal environmental impact, solar chimney power plants have drawbacks, including low efficiency and interruptions during nighttime and cloudy conditions. Improving the collector, which constitutes a significant portion of the system's investment and losses, can make these power plants more cost-effective and competitive. Extensive research has focused on improving collector performance and integrating solar chimneys with other technologies such as photovoltaic panels, geothermal heat, and wind farms to increase electricity generation. However, achieving uninterrupted electricity production during nights, rainy, and cloudy hours remain a significant challenge for solar chimneys. In this study, the objective is to enhance the design of solar chimney collectors to significantly increase the efficiency of solar chimneys compared to conventional designs. Furthermore, we aim to harness stored thermal energy within the collector to ensure uninterrupted electricity generation during nighttime, cloudy, and rainy conditions. **Figure 1** shows the schematic of a solar chimney power plant.

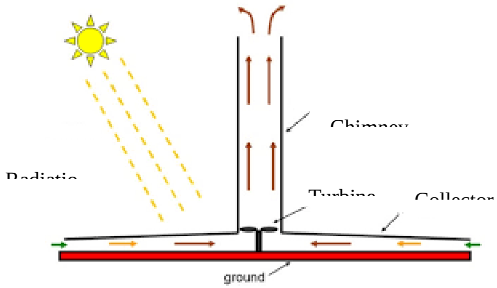

Figure 1. Schematic of a solar chimney power plant

By researching and improving the material and slope of the canopy, configuring and enhancing the collector, the efficiency of these systems can be increased, making investment in them more attractive. To address this challenge, we have decided to enhance the performance of solar collectors for their superior performance among conventional collectors. This involves studying the effects of various parameters on the collector's performance and exploring innovative designs and configurations.

The primary component of a solar chimney power plant is the solar collector, composed of an absorber and a transparent canopy. Numerous parameters significantly influence the collector's performance. Regarding the design of a new counterflow collector, results indicate that air flow velocity and pressure drop at the chimney inlet have the most substantial impact on efficiency (Nasraoui *et al.*, 2020). Al-Kayiem *et al*. (2019) investigated a simple solar chimney with hot gas channels, focusing on improving collector performance through material selection, geometry considerations, plant location, collector slope, environmental conditions, and solar irradiance access. They stated that the collector accounts for approximately 50% of solar power plant investment and system losses. Enhancing this component can make solar chimney investments cost-effective, attractive, and competitive. Ismaili et al. conducted research on strengthening the collector's canopy, slope, and configuration, also introducing a new collector design with branching gears to reduce airflow friction losses inside the collector (Esmaili *et al.*, 2022). Hussam *et al*. (2022) also proposed upgrading the power plant's collector by adding a secondary roof or canopy and dividing the collector into upper and lower sections. The proposed collector regulating mechanism-controlled energy conservation by closing the lower section when less power was required, thereby storing thermal energy in the ground collector. When more power was needed, the lower section opened, allowing airflow under the secondary roof, where it heated up due to ground heat, thereby increasing power generation.

The second component of the solar chimney collector is the ground. This part serves as the average absorber for solar radiation and heat storage. Some researchers have endeavored to enhance the performance efficiency by utilizing the ground as a heat storage medium without phase change. Kazemi *et al*. (2022) studied the unstable behavior of the collector using multi-layer energy storage. Rahdan *et al*. (2021) investigated the impact of ground temperature on solar chimney performance. Cao *et al*. (2021) examined the influence of air temperature on collector arrangement with the ground, while Huang *et al*. (2020) studied and reported upgraded collector data using multi-layer asphalt coating. Additionally, Mehranfar *et al*. (2022) proposed using water bags in the ground collector. Tawalbeh *et al*. (2023) also examined the adverse effects of wind on solar collectors. Pascual-Muñoz *et al*. (2013) suggested integrating a conventional solar chimney technique with another source that may maintain energy input in the absence of solar sources, also investigating a new power plant design using a solar chimney with solid oxide fuel cells. Hafizh *et al*. (2020) developed an integrated mathematical model to simulate the updraft velocity and temperature of airflow inside a small-scale solar updraft power generator. Meanwhile, Yazdi *et al*. (2021) studied a hybrid solar chimney system, applying the turbine effect during different daytime hours and with various heat sources at night.

As observed, extensive research has focused on improving collector performance and integrating solar chimneys with technologies such as photovoltaic panels, geothermal heat, and wind farms to increase electricity generation. However, achieving uninterrupted electricity production during nights, rainy, and cloudy hours remain a significant challenge for solar chimneys. To address this, the study aims to enhance the performance of solar collectors for their superior performance among conventional collectors.

2. Materials and Methods

2.1. Governing Equations

The flow inside the solar chimney is described by the Navier-Stokes equations, including continuity, momentum, and energy transfer equations, written as follows:

2.1.1. Continuity Equation

$$\frac{\partial \rho}{\partial t} + \nabla.\left(\rho\vec{V}\right) = 0 \quad (1)$$

Here, ρ represents density and $\vec{V}$ represents velocity.

2.1.2. Momentum Equation

$$\frac{\partial \rho\vec{V}}{\partial t} + \nabla.(\rho\vec{V}.\overrightarrow{V}) = \nabla.(\tau) - \nabla.(P) + \rho\beta(T - T_{ref})\vec{g} \quad (2)$$

In these equations, we use the Boussinesq approximation where P is the static pressure, I is the unit tensor, and T_{ref} is the reference temperature. The stress tensor T is calculated from the formula:

$$\bar{\bar{\tau}} = \mu(\nabla.\vec{V} + \left(\nabla.\vec{V}\right)^t) - \frac{2}{3}(\nabla.\vec{V})I \quad (3)$$

2.1.3. Energy Equation

$$\frac{\partial \rho E}{\partial t} + \nabla.\left(\rho(E+P)\vec{V}\right) = \nabla.\ \left(\lambda_{eff}\nabla T - \sum h_j\vec{J_j} + \tau\vec{V}\right) + S \quad (4)$$

Here, E represents the total energy, λ is the effective thermal conductivity, h_j denotes various flow terms, and S is the heat source. The Solar Load model, available in Fluent software, is used to determine these parameters.

2.1.4. Discrete Ordinates (DO) Model

The Discrete Ordinates model is used to calculate the solar radiation incident on the semi-transparent collector walls of the solar chimney. The DO model considers the transparency of the collector material and is suitable for calculating heat transfer in solar chimneys. It is expressed as:

$$\nabla.(I_\lambda(\vec{r},\vec{s})\vec{s}) + (a_\lambda,\sigma_s)I_\lambda(\vec{r},\vec{s}) = a_\lambda n^2 I_{b\lambda} + \frac{\sigma_s}{4\pi}\int_0^{4\pi} I_\lambda(\vec{r},\vec{s}')\phi(\vec{s},\vec{s}')d\phi' \quad (5)$$

where ∇ is the operator indicating divergence, $I_\lambda(\vec{r},\vec{s})$ is the spectral intensity at wavelength λ as a function of position r and direction s, s is the direction vector, a_λ is the spectral absorption coefficient, σ_s is the scattering coefficient, n is the refractive index, $I_{b\lambda}$ is the black body emissivity at wavelength λ, ϕ(s,s′) is the phase function describing the probability of scattering from direction s′ to s, and dϕ′ is the differential solid angle.

The total intensity in the direction of $\vec{s}$ is equal to the spectral intensity at the wavelength, which is:

$$I(\vec{r},\vec{s}) = \sum_k I_{\lambda_k}(\vec{r},\vec{s})\Delta\lambda_k \tag{6}$$

The equation $I(\vec{r},\vec{s})$ represents the total intensity I at a given position r and direction s as the sum of the spectral intensities I_{λ_k} over discrete wavelength intervals $\Delta\lambda_k$.

2.1.5. Total Efficiency of the Collector

The overall efficiency of the collector is commonly approximated by the formula:

$$\eta_c = \frac{\dot{m}c_p\Delta T}{G\pi(R_c^2 - R_{ch}^2)} \tag{7}$$

Here, $\dot{m}$ is the mass flow rate of the air, c_p is the specific heat capacity of the air at constant pressure, ΔT is the temperature difference of the air as it passes through the collector, G is the solar radiation flux, R_c is the outer radiu s of the solar collector, and R_{ch} is the inner radius of the solar collector.

These equations and models form the basis for analyzing and optimizing the performance of solar chimneys in generating electricity efficiently under various environmental conditions.

2.2. Validation

Figure 2 shows the counterflow solar chimney collector by Nasraoui *et al.* (2020). In the counterflow collector, the air initially flows over the top part of the collector and then changes direction upon reaching the curved section, entering the lower part and moving in the opposite direction towards the collector's outlet.

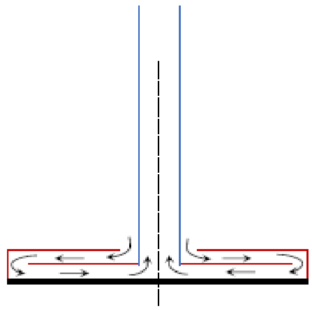

Figure 2. Counterflow solar chimney collector

Figure 3 illustrates the schematic of the counterflow collector. The heights of the upper and lower roofs are considered equal. The dimensions of the collector's inlet, collector radius, chimney radius, upper roof height, and lower roof height are provided in **Table 1**.

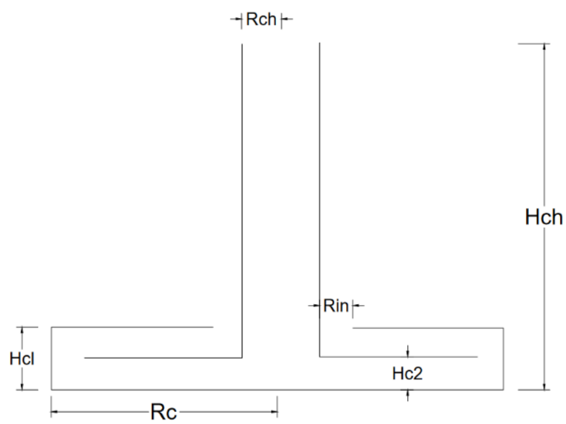

Figure 3. 2D geometry of the counterflow collector

Table 1. Dimensions of the counterflow collector

Inlet Size	Collector Radius	Chimney Radius	Upper Roof Height	Lower Roof Heit	Unit
0.08	1.85	0.36	0.1	0.05	m

As shown in **Figure 4**, an unstructured grid was used for meshing the chimney model for validation, while a structured grid was used inside the pipes to increase the accuracy of the calculations. Due to the complex geometry, the number of elements reached 4,184,795 to ensure both grid independence and high meshing accuracy. The quality of the grid was 0.15, which is considered satisfactory.

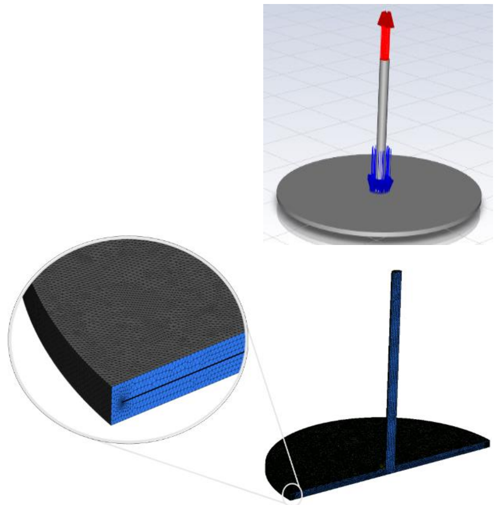

Figure 4. Solar chimney modeling (validation model)

For validation, the results from Nasraoui *et al.* (2020) were used. **Figure 5** shows the validation values of velocity changes along the solar chimney. The velocity values at the collector outlet were obtained as 2.83 m/s, which compared to the actual value of 2.8 m/s, shows an error of 1.06%, indicating the high accuracy of the calculations performed.

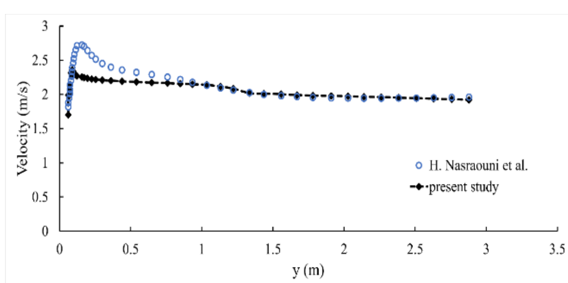

Figure 5. Velocity along the chimney

2.3. Simulation

After simulating the counter-flow solar chimney collector, we introduce an innovation. To this end, we embedded pipes with a diameter of 0.03 m containing steam at 116°C in a quarter-circle arrangement within the collector. This setup is intended to serve as an additional heat source to warm the air inside the collector. As shown in **Figures 6** and **7**, the new collector geometry, with two inlets and two outlets for hot steam, heats the air more effectively than solar radiation alone and acts as an additional heat source.

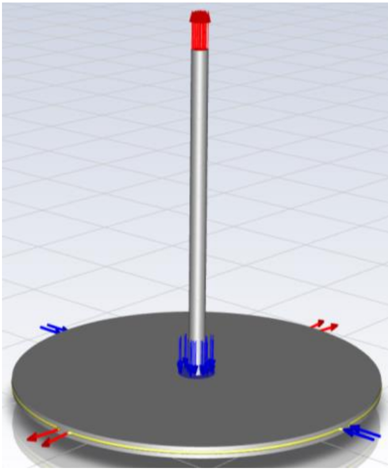

Figure 6. Solar chimney modeled with additional heat source

3. Results and Discussion

Figure 7 illustrates the velocity distribution at three different times (08:00, 13:00, and 21:00) in a collector with and without an additional heat source. A detailed analysis of these graphs highlights the following points:

At all times (08:00, 13:00, and 21:00), the presence of an additional heat source (represented by red curves) leads to an increase in the fluid velocity at various points within the collector compared to the state without an additional heat source (represented by blue curves). This velocity increase is due to the rise in the kinetic energy of the fluid influenced by the additional heat source. The additional heat source transfers more heat to the fluid, increasing its temperature and consequently reducing its density. This results in increased fluid flow due to pressure and temperature differences.

At all three times examined, it is observed that the fluid velocity increases as it moves towards the collector's outlet after entering. This increase in velocity indicates the acceleration of the fluid flow due to the reduction in cross-sectional area and the increase in kinetic energy caused by heating. Around a radius of approximately 1.8 m, where the hot gas pipes are located, a momentary increase in velocity is observed. This momentary increase is due to the higher heat transfer from the hot gas pipes to the fluid, which results in increased kinetic energy and, consequently, higher velocity.

In all three times examined, it is observed that the fluid velocity increases as it approaches the chimney's inlet and reaches its maximum at the chimney's inlet. This increase in velocity indicates the enhanced fluid flow due to pressure and temperature differences near the chimney's inlet. The maximum velocity at the chimney's inlet is due to the convergence of the fluid flow at this point and the pressure changes caused by temperature and velocity differences along the collector.

The presented graphs show that the additional heat source has a significant impact on increasing the fluid velocity along the collector, and this effect varies at different points within the collector. The increase in fluid velocity is due to the rise in kinetic energy resulting from the higher heat transfer to the fluid. Additionally, the velocity distribution along the collector indicates an increase in velocity as it approaches the chimney's inlet, reflecting the pressure and temperature changes along the collector.

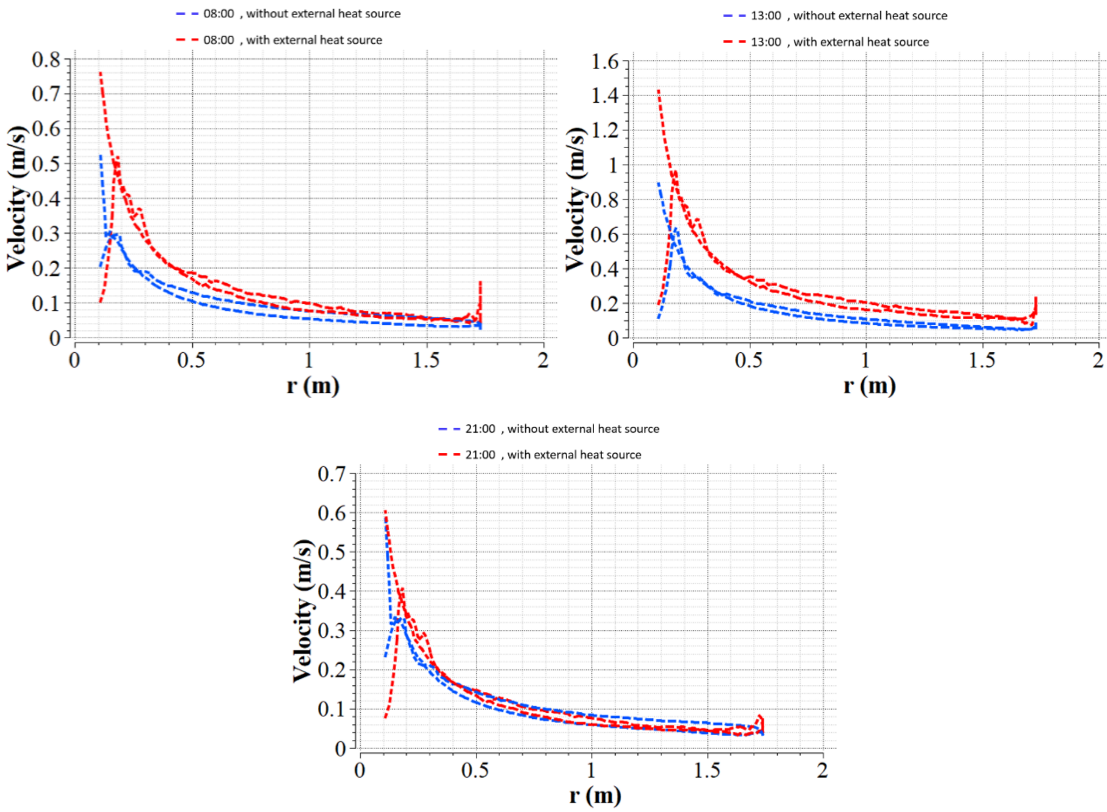

Figure 7. Velocity along the collector

Figure 8 illustrates the fluid velocity distribution along the collector at three different times (08:00, 13:00, and 21:00) with an additional heat source. The curves show that the velocity distribution follows a similar pattern at all three times but with different velocity magnitudes.

At 13:00 (red curve), the fluid velocity reaches its maximum value, indicating the significant impact of the external heat source in increasing fluid speed. This increase is due to the maximum solar radiation at this time, which raises the fluid temperature and decreases its density, resulting in higher fluid velocity. Conversely, at 21:00 (green curve), the fluid velocity is at its lowest, reflecting the reduced impact of the external heat source. With decreased solar radiation, the fluid temperature is lower than at other times, leading to a lower velocity. At 08:00 (blue curve), the fluid velocity is between the values observed at 13:00 and 21:00, indicating a moderate impact of the external heat source. This time of day marks the beginning of increasing solar radiation.

At all three times, the fluid velocity increases after entering the collector and moving towards the outlet. This acceleration is due to the reduction in cross-sectional area and the increase in kinetic energy caused by heating. Around a radius of approximately 1.8 m, where the hot gas pipes are located, a momentary increase in velocity is observed. This increase is due to the higher heat transfer from the hot gas pipes to the fluid, which raises the kinetic energy and, consequently, the velocity.

As the fluid approaches the chimney inlet, its velocity increases and reaches a maximum. This acceleration is due to the enhanced fluid flow resulting from pressure and temperature differences near the chimney inlet. The maximum velocity at the chimney inlet is due to the convergence of the fluid flow at this point and the pressure changes caused by temperature and velocity differences along the collector.

The highest fluid velocity is observed at 13:00, indicating the significant impact of the heat source at this time, likely due to increased solar radiation. At 08:00, the fluid velocity is relatively high but less than at 13:00, marking the start of increased solar radiation. At 21:00, the fluid velocity is significantly lower than at the other times, likely due to decreased solar radiation and lower fluid temperatures.

These results demonstrate that the impact of the external heat source on increasing fluid velocity along the collector is highly time-dependent, with the maximum effect occurring when the sun is at its peak (13:00). The additional heat source significantly enhances the kinetic energy of the fluid, resulting in higher velocities and improved performance of the solar chimney system.

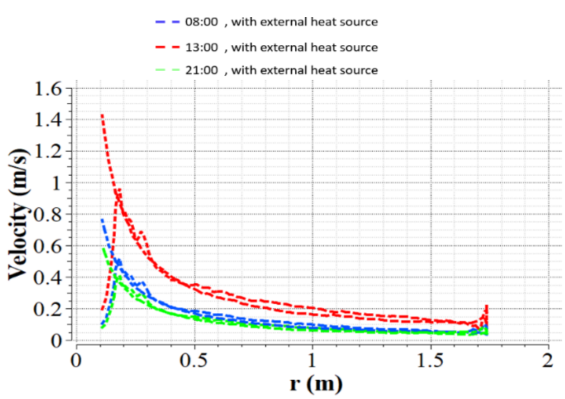

Figure 8. Velocity along the collector axis for every 3 hours

To determine the efficiency of the solar chimney, we use formula (7), and the results are presented in **Table 2**. As seen in **Table 2**, the efficiency with an additional heat source shows a significant increase compared to the case without an additional heat source. There is an approximately 10.9%

increase at 8 AM and a 32% increase at 1 PM. Comparing the efficiency at 8 AM and 1 PM, we observe a 40% difference with the additional heat source and an 18% difference without it. This can be attributed to both the intensity and direction of solar radiation. When comparing the solar radiation intensity at 8 AM and 1 PM, the difference in intensity is relatively small compared to the difference in efficiency, highlighting the importance of the direction of sunlight. At 1 PM, the sun directly hits the collector's roof, heating the air inside the collector more effectively. At 9 PM, without an additional heat source, the efficiency is zero due to the absence of solar radiation. By adding an external heat source to the solar chimney, the flow speed within the system increases significantly, enhancing overall efficiency. The highest efficiency is observed at noon due to optimal sunlight direction and intensity. This method enables continuous electricity production, even at night, transforming the solar chimney into a more reliable and efficient power generation system.

Table 2. Collector efficiency for different hours

Hour	**Solar Radiation Intensity (W/m^2)**	**Collector Efficiency without Heat Source (%)**	**Collector Efficiency with Heat Source (%)**
8	716.91	0.181492	11.0165
13	880	18.2991	51.2513
21	0	-	-

4. Conclusion

In this study, a novel collector design is proposed that not only heats the air under the collector through solar radiation but also utilizes an auxiliary heat source to further raise the air temperature. This temperature increase accelerates the airflow, which subsequently enhances turbine rotation and consequently boosts electricity generation. The results of this study demonstrate that incorporating an external heat source into the chimney significantly increases the flow speed within the system. The air accelerates more rapidly towards the collector's outlet, entering the chimney at a higher speed, which in turn enhances electricity production by increasing the rotation of the wind turbine through the generator. This method allows for continuous electricity production, even during nighttime hours. For the future work, the concept of a photovoltaic solar chimney (PV/SC) can be used to enhance the efficiency of our hybrid solar system. As air moves up and down the solar cells, it cools the panels, resulting in increased photovoltaic (PV) electrical efficiency.

Acknowledgement

The authors would like to thank the New Energy Research Group at New Materials Technology and Processing Research Center, Islamic Azad University, Neyshabur Branch for supporting the research of this study.

Credit Author Statement

Supervision and project administration, Yazdi, M.H.; conceptualization and methodology, Yazdi, M.H.; software and validation, Yazdi, M.H.; investigation, Yazdi, M.H., Mahrooghi, A., Zarandi, O.; writing—original draft preparation, Yazdi, M.H., Mahrooghi, A.; writing—review and editing, Mahrooghi, A.

Conflicts of Interest

The authors declare no conflict of interest.

References

Al-Kayiem, H.H., Aurybi, M.A., Gilani, S.I., Ismaeel, A.A., & Mohammad, S.T. (2019). Performance evaluation of hybrid solar chimney for uninterrupted power generation. *Energy*, 166, 490-505.

Cao, Y., Pourhedayat, S., Dizaji, H.S., & Wae-hayee, M. (2021). A comprehensive optimization of phase change material in hybrid application with solar chimney and photovoltaic panel for simultaneous power production and air ventilation. *Building and Environment*, 197, 107833.

Esmaili, M.M., Fallah, S.H., Izanlu, M., & Valipour, M.S. (2022). Investigation on the performance of a solar chimney-flare gas hybrid system. *Sustainable Energy Technologies and Assessments*, 52, 102279.

Hafizh, H., Fudholi, A., Yazdi, M.H., & Ridwan, A. (2020). Mathematical modeling and aerothermal simulation of a small-scale solar updraft power generator. *International Journal of Renewable Energy Research (IJRER)*, 10(4), 1655-1663.

Huang, M.H., Chen, L., Lei, L., He, P., Cao, J.J., He, Y.L., Feng, Z.P., & Tao, W.Q. (2020). Experimental and numerical studies for applying hybrid solar chimney and photovoltaic system to the solar-assisted air cleaning system. *Applied Energy*, 269, 115150.

Hussam, W.K., Salem, H.J., Redha, A.M., Khlefat, A.M., & Al Khatib, F. (2022). Experimental and numerical investigation on a hybrid solar chimney-photovoltaic system for power generation in Kuwait. *Energy Conversion and Management: X*, 15, 100249.

Kazemi, K., Ebrahimi, M., Lahonian, M., & Babamiri, A. (2022). Micro-scale heat and electricity generation by a hybrid solar collector-chimney, thermoelectric, and wind turbine. *Sustainable Energy Technologies and Assessments*, 53, 102394.

Mehranfar, S., Gharehghani, A., Azizi, A., Andwari, A.M., Pesyridis, A., & Jouhara, H. (2022). Comparative assessment of innovative methods to improve solar chimney power plant efficiency. *Sustainable Energy Technologies and Assessments*, 49, 101807.

Nasraoui, H., Driss, Z., & Kchaou, H. (2020). Novel collector design for enhancing the performance of solar chimney power plant. *Renewable Energy*, 145, 1658-1671.

Pascual-Muñoz, P., Castro-Fresno, D., Serrano-Bravo, P., & Alonso-Estébanez, A. (2013). Thermal and hydraulic analysis of multilayered asphalt pavements as active solar collectors. *Applied Energy*, 111, 324-332.

Rahdan, P., Kasaeian, A., & Yan, W.M. (2021). Simulation and geometric optimization of a hybrid system of solar chimney and water desalination. *Energy Conversion and Management*, 243, 114291.

Tawalbeh, M., Mohammed, S., Alnaqbi, A., Alshehhi, S., & Al-Othman, A. (2023). Analysis for hybrid photovoltaic/solar chimney seawater desalination plant: a CFD simulation in Sharjah, United Arab Emirates. *Renewable Energy*, 202, 667-68.

Yazdi, M.H., Solomin, E., Fudholi, A., Sopian, K., & Chong, P.L. (2021). Numerical analysis of the performance of a hybrid solar chimney system with an integrated external thermal source. *Thermal Science and Engineering Progress*, 26, 101127.